The Astronomical Journal, 165:220 (7pp), 2023 June https://doi.org/10.3847/1538-3881/acca19

Spectroscopic Orbits of Subsystems in Multiple Stars. X (Summary)

Andrei Tokovinin
Cerro Tololo Inter-American Observatory—NSF's NOIRLab Casilla 603, La Serena, Chile; andrei.tokovinin@noirlab.edu
Received 2022 December 16; revised 2023 March 31; accepted 2023 April 2; published 2023 May 2

Abstract

Results of a large program of spectroscopic monitoring of nearby solar-type stellar hierarchical systems using the CHIRON echelle spectrograph at the 1.5 m telescope are summarized. Ten papers of this series contain 102 spectroscopic orbits and substantially contribute to the knowledge of periods and eccentricities, providing input for the study of their formation and early evolution. Radial velocities of an additional 91 targets without CHIRON orbits (members of wide physical pairs) are published here. Our results are compared to the recent Gaia nonsingle star (NSS) catalog, revealing its strengths and weaknesses. The NSS provides orbital periods for 31 objects of the CHIRON sample (about one third). Of the 22 spectroscopic NSS orbits in common, 14 are in good agreement with CHIRON, the rest have reduced velocity amplitudes or other problems. Hence ground-based monitoring gives, so far, a more accurate and complete picture of nearby hierarchies than Gaia. The distribution of inner periods in hierarchical systems is nonmonotonic, showing a shallow minimum in the 30–100 days bin and a strong excess at shorter periods, compared to the smooth distribution of simple binaries in the field. The period-eccentricity diagram of inner subsystems updated by this survey, recent literature, and Gaia, displays an interesting structure.

Unified Astronomy Thesaurus concepts: Spectroscopic binary stars (1557); Multiple stars (1081); Visual binary stars (1777); Radial velocity (1332)

Supporting material: machine-readable tables

1. Introduction

Observations of spectroscopic subsystems in nearby solar-type stars are motivated by the desire to complement statistics of hierachies in the solar neighborhood (Tokovinin 2014a). In most cases, discovery of such subsystems by variable radial velocity (RV) or astrometric acceleration has not been followed by determination of the orbits. Without knowledge of periods and mass ratios, statistical distributions remain poorly constrained, hence useless as input for testing models of formation and early evolution of hierarchies. Development of predictive models of stellar multiplitity remains the ultimate goal that justifies new observations.

Monitoring of RVs is a classical way to find periods, mass ratios, and orbital eccentricities. Such long-term programs have been conducted since 2015 at the 1.5 m telescope at Cerro Tololo with the CHIRON high-resolution optical echelle spectrograph (Tokovinin et al. 2013). Its main targets were solar-type stars within 67 pc belonging to hierarchical systems with three or more components. The program has been complemented by hierarchies at larger distances, also with solar-type components. Short-period orbits could be determined rapidly, while longer periods required observations for several years. The resulting orbits accompanied by discussions of each hierarchy were published in a series of 10 papers listed in Table 1, with a total of 102 spectroscopic orbits determined throughout this program. A summary of this effort is provided here.

The classical approach of monitoring selected objects from the ground is nowadays complemented by the large spectroscopic surveys, e.g., GALAH (Buder et al. 2021) and LAMOST (Cui et al. 2012), and by the Gaia space mission (Gaia Collaboration et al. 2021). The Gaia Data Release 3 (GDR3) includes a catalog of nonsingle stars (NSS), which contains about 3×10^5 spectroscopic and/or astrometric orbits (Gaia Collaboration et al. 2022). Uniformity of the Gaia coverage, compared to the selective object-by-object study, is a huge advantage for the statistics. However, the current NSS suffers from incompleteness and selection and contains a nonnegligible fraction of wrong orbits, as noted by its compilers (Pourbaix et al. 2022). I compare here the NSS and CHIRON orbits to highlight the advantages and caveats of both approaches. Taken together, the ground- and space-based orbits substantially complement our knowledge of stellar hierarchies and their architecture. Some statistical results are presented here based on the current version of the Multiple Star Catalog (MSC; Tokovinin 2018a) that can be accessed online.[1]

The CHIRON multiplicity project is part of a larger observational effort. Studies of stellar hierarchies on the northern sky using a correlation radial-velocity meter were conducted in the 1990s, as summarized by Tokovinin & Smekhov (2002), and continued in the following decades in a series of papers by Tokovinin & Gorynya (2001, 2007) and Gorynya & Tokovinin (2014, 2018). In parallel, high-resolution imaging of wider (mostly astrometric) subsystems using adaptive optics and speckle interferometry was undertaken (Tokovinin et al. 2010, 2012); it is continued at present. With all techniques (including Gaia) combined, a wide and deep coverage of the full parameter space can be achieved for nearby stars.

The CHIRON sample is presented in Section 2 and the orbits are compared to the Gaia orbits in Section 3. In Section 4, RVs of other targets (mostly wide visual binaries) measured with CHIRON are published for future use. The period distribution

[1] http://www.ctio.noirlab.edu/~atokovin/stars/ and http://vizier.u-strasbg.fr/viz-bin/VizieR-4?-source=J/ApJS/235/6

Table 1
Publications on the CHIRON Survey

Paper[a]	Bibcode	N_{sys}	N_{orb}
1	2016AJ....152...11T	4	7
2	2016AJ....152...10T	4	7
3	2018AJ....156...48T	6	9
4	2018AJ....156..194T	9	10
5	2019AJ....157...91T	9	9
6	2019AJ....158..222T	11	12
6a	2020AJ....159...88T	1	2
7	2020AJ....160...69T	8	12
8	2022AJ....163..161T	10	19
9	2023AJ....165..160T	14	15

Note.
[a] References: 1—Tokovinin (2016a); 2—Tokovinin (2016b); 3—Tokovinin (2018b); 4—Tokovinin (2018c); 5—Tokovinin (2019a); 6—Tokovinin (2019b); 6a—Tokovinin (2020a); 7—Tokovinin (2020b); 8—Tokovinin (2022); 9 - Tokovinin (2023).

and the $P-e$ diagram are discussed briefly in Section 5, and the summary is given in Section 6.

2. Overview of the CHIRON Program

The main 67 pc sample of hierarchies with solar-type primary stars was based on the Hipparcos catalog (Tokovinin 2014b), so it is convenient to use here Hipparcos (HIP) numbers as primary identifiers. I extracted from the database of CHIRON observations all Hipparcos stars relevant to this project, omitting a few systems which are not in Hipparcos. Table 2 lists 120 individual targets (resolved or blended components of multiple systems) featured here. The columns contain the HIP number, MSC/WDS code based on the J2000 coordinates, component identifier, its equatorial coordinates for J2000, V magnitude, parallax ϖ, its source, the orbital period P determined in this project, and the orbit reference (the paper number). In some cases the components of a multiple system have individual HIP numbers (e.g., HIP 6868 and 6873); otherwise, the secondary stars are identified here by the HIP number of the primary and a component letter (e.g., HIP 24320 A and B). Detailed information on all components (accurate coordinates, proper motions, etc.) can be found in the MSC. As indicated in the parallax reference column, most parallaxes come from the GDR3 or its NSS extension (DR3N). If parallax of the component is not measured in GDR3, parallax of other system's components is used instead (DR3*). If there are no wide components, the parallax comes from HIP or visual orbits (dyn and orb). The median parallax of the CHIRON sample is 17.3 mas, 85 targets are within 67 pc (parallaxes above 15 mas). Four targets are revealed as spectroscopic triples with inner periods of a few days and outer periods on the order of a year (HIP 11537A, 27970A, 56282A, 111598A); both spectroscopic periods are listed for those stars, which also have outer visual companions (they are rare quadruples of 3+1 hierarchy).

Candidates for determination of spectroscopic orbits were mostly identified in the survey by Nordström et al. (2004) and in other publications as components of visual binaries with variable RVs. They are featured in the original 67 pc sample as hierarchies with unknown inner periods. Some of these stars also have astrometric accelerations (the astrometric and spectroscopic binaries overlap).

Measurements of the RVs of wide (resolved) nearby binaries with the fiber echelle and CHIRON spectrographs at the CTIO 1.5 m telescope are reported in (Tokovinin 2015). The aim was to detect new subsystems (one measurement of a substantial RV difference between the components is sufficient for a detection). This minisurvey of 96 wide pairs revealed 17 new subsystems which were added to the present program. Components of additional wide multiples were episodically observed with CHIRON in the following years as a complement to the main program; their RVs are reported here in Section 4. Typically, components of wide pairs were observed only once.

The goal of our survey was to determine all (or most) periods up to 1000 days. Naturally, some periods turned out to be longer than this arbitrary threshold. The distribution of orbital periods determined in this survey is plotted in Figure 1 in dashed line. For comparison, the distribution of periods in all known inner subsystems in hierarchies within 67 pc with primary star masses from 0.5 to 1.5 $M_{\odot}$ is plotted. The dotted line traces the standard log-normal period distribution of field binaries with a median of 10^5 days and a logarithmic dispersion of 2.28 dex (Raghavan et al. 2010). At $P>100$ days, both distributions are similar, showing an increase of orbits with longer periods. However, inner subsystems have a strong excess of orbits with $P<30$ days compared to the canonical log-normal curve. In other words, short-period binaries have a strong preference to belong to hierarchical systems. This phenomenon is further discussed below in Section 5.2. Neither the MSC nor the CHIRON samples are complete, but, owing to the extended monitoring, periods shorter than 10^3 days should be represented uniformly. So, the excess of short periods and the local minimum in the 30–100 days bin are real features rather than selection effects.

3. Comparison between CHIRON and Gaia NSS Orbits

The number of spectroscopic orbits in GDR3/NSS (1.8×10^5) overwhelms all spectroscopic orbits determined to date from the ground: on 2020 March 24, the SB9 catalog[2] (Pourbaix et al. 2004) contained only 4004 systems, with 2/3 of those on the northern sky. Gaia determined orbits by an impersonal automated procedure (Gaia Collaboration et al. 2022; Pourbaix et al. 2022). The duration of the GDR3 mission (34 months) and the observing cadence set by the Gaia scanning law naturally restrict the range of accessible orbits. Most Gaia periods are under 1000 days, and orbital periods close to one year and its harmonics are underrepresented. The distribution of Gaia orbits on the sky is nonuniform and clearly shows an imprint of the scanning law. Candidates for Gaia orbit determination went through a vetting procedure (visual binaries with close separations were rejected), and the orbits were checked by various filters. Documentation available on the Gaia website (Pourbaix et al. 2022) describes the vetting and quality control. Comparison with known spectroscopic orbits in the cited document indicated a "recovery rate" (correctness) of Gaia spectroscopic orbits between 0.7 and 0.9, depending on the comparison sample and criteria used.

The CHIRON sample presented here was matched by coordinates to the Gaia catalogs of single- and double-lined spectroscopic orbits (SB1 and SB2, respectively) and other NSS solutions. Coordinate search reveals 31 Gaia orbits among

[2] https://sb9.astro.ulb.ac.be/

Table 2
Main CHIRON Sample (Fragment)

HIP	WDS (J2000)	Comp.	R.A. (deg)	Decl. (deg)	V (mag)	ϖ (mas)	References plx[a]	P (days)	SB[b]	References
1103	00138+0812	A	3.440421	8.193534	7.40	13.19	DR3	…	0	…
2863	00363−3818	A	9.073152	−38.294137	8.36	9.56	DR2	4.81	2	5
3150	00400+1016	A	10.009878	10.266985	8.71	5.99	DR3	172.5	2	7
3645	00467−0426	A	11.668998	−4.427128	7.58	30.08	DR3	1530.9	2	9
4974	01037−3024	B	15.932681	−30.398708	8.78	6.40	DR3	14.71	2	5
6868	01284+0758	A	22.095514	7.961353	6.21	8.47	DR3	…	0	7
6873	01284+0758	B	22.114598	7.958176	8.04	8.13	DR3	115.6	2	7

Notes.
[a] Parallax references: DR3—Gaia Data Release 3; DR3N—Gaia Data Release 3, NSS catalog; DR3*—Gaia Data Release 3, other component of the system; HIP — Hipparcos; dyn —dynamical (visual orbit and mass); orb —orbital (visual-spectroscopic orbit).
[b] SB orbit flags: 0—no orbit; 1—single-lined orbit; 2—double-lined orbit.

(This table is available in its entirety in machine-readable form.)

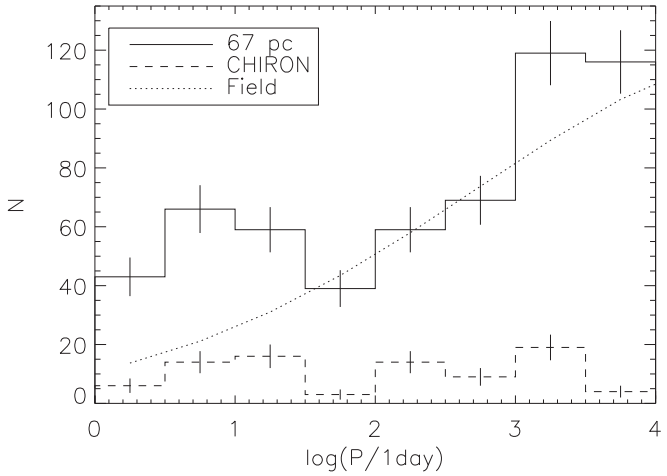

Figure 1. Histogram of inner periods in hierarchical systems of solar-type stars within 67 pc (full line) and of the subset of 90 inner periods resulting from the CHIRON program (dashed line). The dotted line is a log-normal period distribution of field solar-type binaries from Raghavan et al. (2010) with arbitrary normalization.

CHIRON targets; four of those have no CHIRON orbits owing to the small number of observations, for five targets NSS contains only astrometric orbits with matching periods. Table 3 compares the CHIRON and NSS orbits for 31 common targets. The NSS solution codes are obvious (SB1 and SB2 for single- and double-lined spectroscopic orbits, ASB1 for spectro-astrometric orbits, and AORB for purely astrometric orbits). One NSS orbit (HIP 21079A) is false owing to the wrongly determined period of 2.71 days (the true period is 217 days). Seven NSS orbits have reduced RV amplitudes, either because of blending with lines of the secondary or because of an inaccurate shape of the NSS RV curve. The remaining 14 SB orbits in common between CHIRON and NSS are in reasonably good mutual agreement. Note, however, that NSS missed some subsystems, either inner (1.56 days in HIP 22531A) or outer with periods exceeding the GDR3 mission duration (in HIP 56282A, 64478A). For HIP 36165 with $P = 2300$ days, Gaia detected so far only the acceleration and the RV trend. Overall, only a third of the CHIRON sample has spectroscopic or astrometric orbits in the NSS. The CHIRON targets are bright (well above the Gaia RV threshold of 13 mag), and most orbital periods are under 1000 days. So, despite the large total number of orbits, the NSS orbit catalog is still very incomplete.

Figure 2 compares CHIRON and Gaia orbits of six common stars where the periods match approximately. Four systems are double-lined in CHIRON, but single-lined in Gaia. When the secondary lines are much fainter than those of the primary (HIP 9148, 22531B), Gaia gives a reasonable match for the primary star with a slightly reduced RV amplitude. For pairs with comparable-mass components (HIP 59426, 81394), the Gaia RV amplitudes are dramatically underestimated; moreover, the shape and phase of the Gaia RV curves are incorrect. For two single-lined binaries (HIP 24320B, 34212), the CHIRON and Gaia orbits are similar (small phase shifts are due to inaccurate Gaia periods). Interestingly, a comparison of the NSS with two large ground-based RV surveys indicated that only about a half of Gaia SB1 orbits could be validated (Bashi et al. 2022).

The availability of Gaia orbits is most welcome. However, it does not make the CHIRON survey obsolete, quite to the contrary. Presently, Gaia provides orbits for only a small fraction of inner subsystems in nearby hierarchies, and some of those orbits are questionable even for the relatively simple binaries shown in Figure 2. More complex and more interesting systems (e.g., triple- and quadruple-lined) can be discovered and studied only by dedicated ground-based programs like this one. Systematic underestimation of RV amplitudes by Gaia due to line blending leads to the underestimated mass ratios, so the use of Gaia orbits for a statistical study of the mass ratio distribution is not recommended.

4. Radial Velocities of Wide Pairs

Wide (resolved) pairs were probed for the presence of subsystems by measuring RVs of each component and looking for substantial differences (Tokovinin 2015). This work has been continued in the following years and its complementary results are reported here. Some wide pairs contain known visual subsystems with long periods, and their RVs change on a timescale of decades. The RV measurements of wide pairs with CHIRON are published in Table 4, to be used in the future for determination of long-period orbits. This table also contains previously unpublished RVs of stars from the main program where insufficient number of observations does not allow for orbit calculation or the orbits are known from other sources. For example, the orbital period of HIP 1103A, 1343 days, is

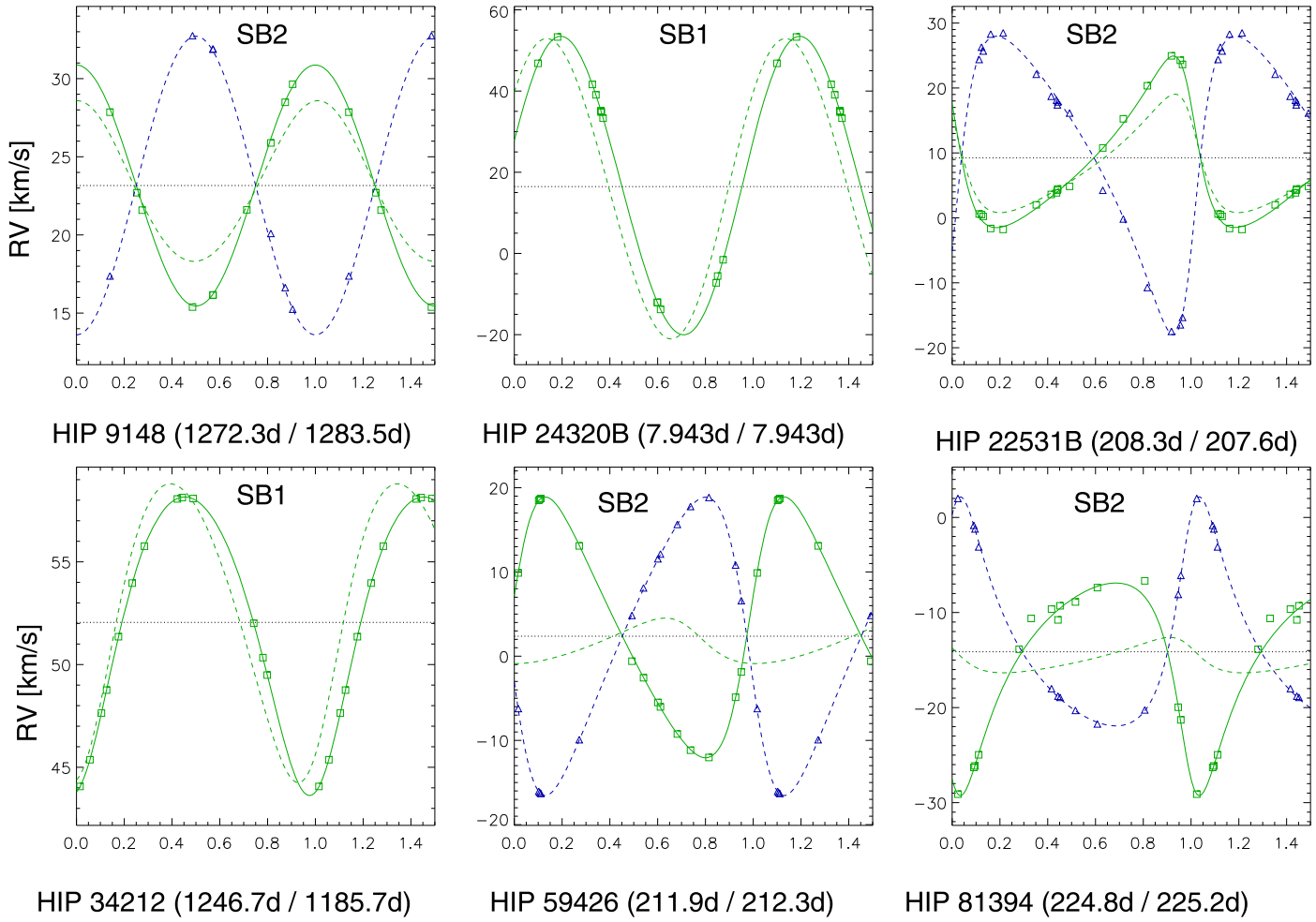

Figure 2. Comparison between six CHIRON and Gaia spectroscopic orbits. All plots show RVs of the primary (solid green line and squares) and secondary (dashed blue line and triangles) components measured by CHIRON vs. orbital phase. The Gaia orbits are depicted by dashed green lines. The CHIRON and Gaia periods are indicated under each plot.

now determined by Gaia, and its continued monitoring with CHIRON makes little sense. Columns of the table identify stars by their HIP number and component letter. Then follow Julian date, RV, amplitude a, and rms width σ of the cross-correlation dip. The dip parameters are helpful in evaluating the RV errors (wide and shallow dips give larger errors), while variable dips indicate blending of several components with variable RVs. Table 4 contains 162 RVs of 91 distinct targets.

Five stars in Table 4 have multi-component dips and deserve individual comments. Triple lines in HIP 49442A were discovered here and indicate a spectroscopic subsystem in this $0\farcs18$ visual pair; the RV of the B component, at $4\farcs4$ from A, was also measured. The double dip of HIP 61465B signals a subsystem, in agreement with the astrometric signature of an unresolved binary in Gaia; its counterpart HIP 61466A at $27\farcs5$ may also contain a subsystem. HIP 78662C (a $V = 8$ mag star at $11''$ from the bright young visual binary HIP 78662AB) may have a double dip, but its large width and small amplitude render this discovery uncertain. The modest RV difference between the dip components in HIP 79588AB may be caused by motion in the 34 yr visual orbit with a large eccentricity of 0.8. HIP 111391AB is also a visual binary with a period of 198 yr and an eccentric orbit which likely causes the small and constant RV difference between the two dip components.

5. Statistics of Inner Subsystems

5.1. Period-eccentricity Diagram

Patient accumulation of data on nearby solar-type hierarchies improves completeness of their sample. The multiyear CHIRON survey and the Gaia DR3 greatly reduce the historic bias in favor of short periods. Although not all inner orbits with $P < 3000$ days are known, the observational "window" is more uniform, and the number of known orbits is larger than a decade ago. So, a fresh look at the statistics in the short-period regime is warranted using the up-to-date MSC.

I selected from the MSC inner subsystems with primary masses from 0.7 to 1.5 $M_\odot$ (solar-type), known periods under 3000 days, and distances within 100 pc—a total of 743 cases with spectroscopic, astrometric, or visual inner orbits (455 ground-based, 288 from Gaia). References to the orbits can be found in the MSC and in SB9 (Pourbaix et al. 2004). The median primary mass is 0.99 $M_\odot$. If the distance limit is reduced to 67 pc, the balance between ground-based (325) and Gaia (53) orbits shifts further, showing improved completeness of the ground-based data for nearby stars.

Figure 3 plots the period-eccentricity relation for inner subsystems within 100 pc. The upper envelope of the points outlines the tidal circularization: most orbits with $P < 10$ days are circular (Meibom & Mathieu 2005). Several crosses at

Table 3
Comparison between CHIRON and Gaia NSS[b] Orbits

HIP	Comp.	SB1/2	P_{CHI} (days)	NSS[a] sol.	P_{NSS} (days)
1103	A	…	…	SB1	1343.0
6873	B	SB2	115.6	SB2	112.4
7852	A	SB1	1177.5	SB1	1184.0
9148	A	SB2	1272.3	ASB1	1283.5[b]
16853	A	…	…	ASB1	204.1
21079	A	SB1	217.0	SB1	2.71[c]
22531	A	SB1	1003	AORB	1000.8
22534	B	SB2	208.3	ASB1	207.6[b]
24320	A	SB1	1430.3	SB1	1042.9
24320	B	SB1	7.943	SB1	7.943
34212	A	SB1	1246.7	SB1	1185.6
35733	A	SB2	4.63	SB2	4.63
51578	A	SB1	2.19	SB1	2.19
56282	A	SB1	121.1	SB1	125.3
57572	A	…	…	ASB1	169.6
59426	A	SB1	211.6	ASB1	212.3[b]
64478	A	SB2	4.23	SB2	4.23
75663	A	SB1	623.8	ASB1	626.7[b]
78163	B	SB1	2082.5	AORB	1532.4
81395	B	SB2	224.8	ASB1	225.2[b]
84789	A	SB2	2.28	SB2	2.28
88728	A	SB1	1132.0	SB1	1267.8[b]
100420	A	SB2	790.6	AORB	805.4
101472	A	SB2	354.9	AORB	354.0
103814	A	SB1	1089.0	ASB1	1119.7
104833	C	SB1	11.34	SB1	11.34
105441	A	SB1	4.62	SB1	4.62
105441	B	…	…	ASB1	549.5
107731	A	SB2	469.9	ASB1	469.3[b]
109443	A	SB1	970.9	SB1	989.8
115552	A	SB2	17.48	SB2	17.48

Notes.
[a] NSS solutions: SB1—single-lined spectroscopic; SB2—double-lined spectroscopic; ASB1—astrometric and single-lined spectroscopic; AORB—astrometric.
[b] Reduced RV amplitude.
[c] Wrong period.

Table 4
RVs of Stars in Wide Pairs (Fragment)

HIP	Comp.	JD −2400000	RV (km s^{-1})	a	σ (km s^{-1})
1103	A	57276.7918	2.785	0.056	20.455
1103	A	57299.7225	2.729	0.057	20.539
1103	A	57333.5715	2.814	0.057	20.569
1103	A	57983.7853	5.967	0.057	20.178
2713	A	57986.7734	8.987	0.353	4.345
2715	C	57986.7745	5.899	0.307	4.730
5896	B	57985.7965	8.228	0.457	4.465
5896	A	57985.7954	8.042	0.036	31.149
6712	A	57985.8439	−23.365	0.471	3.844

(This table is available in its entirety in machine-readable form.)

$P < 10$ days, outside the envelope, are Gaia orbits with spurious periods that should be ignored. The large number of orbits reveals an interesting structure in this diagram, such as two concentrations of eccentric orbits with periods of 10–30 days and with $P > 100$ days, while the number of orbits in the intermediate 30–100 days interval appears smaller and these orbits seem to have smaller eccentricities. Circular orbits reappear again at $P > 1000$ days.

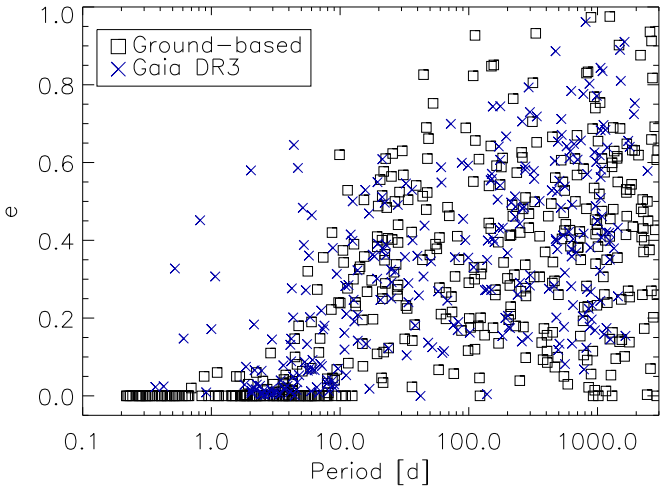

Figure 3. Periods and eccentricities of 743 inner subsystems with solar-type components found in the MSC. Squares correspond to the ground-based orbits, blue crosses are orbits from Gaia NSS.

Period-eccentricity diagrams for spectroscopic binaries can be found in many papers (e.g., Raghavan et al. 2010; Triaud et al. 2017; Price-Whelan et al. 2020; Torres et al. 2021); a circularization period $P_{\rm circ}$ between 7 and 10 days is inferred from these plots. A few eccentric orbits with periods shorter than $P_{\rm circ}$ seen in such diagrams are explained by inefficient tides in stars with primary masses above 1.3 $M_\odot$ and small secondaries (Triaud et al. 2017) or by the influence of tertiary companions (Mazeh 1990); all close binaries in Figure 3 are inner subsystems within multiple stars. Most short-period eccentric orbits derived by Price-Whelan et al. (2020) "in the regime of sparse, noisy, and poorly sampled multiepoch data" likely are spurious.

All binaries with periods less than ∼10 yr were formed by some kind of migration, although the migration mechanisms are still under debate (Moe & Kratter 2018). The $P - e$ diagram may be instructive from this perspectuve. It shows that some inner pairs with $P > 1000$ days could be formed with quasicircular orbits (many visual binaries with nearly circular orbits and periods on the order of a decade are known as well). However, further shortening of the period seems to be associated with an eccentricity growth, given that small eccentricites are rare at periods of $\sim 10^2$ days. The mechanism responsible for migration in this regime should be associated with a loss of angular momentum, e.g., via interaction with a circumbinary disk or with outer companions. The growing eccentricity and shortening period eventually bring the pair into a regime of tidal circularization, where separation at periastron is a few stellar radii. Concentration of points at $P \sim 20$ days and $e = 0.4 \ldots 0.6$ in Figure 3 corresponds to inner pairs that have reached the tidal regime and apparently start slow evolution toward shorter periods and circular orbits. Interestingly, D'Orazio & Duffell (2021) found by hydrodynamical simulation that an eccentric binary in a coplanar prograde disk evolves to shorter periods, while eccentrity fluctuates around the $e = 0.4$ attractor; in contrast, a binary with $e < 0.1$ does not migrate and its orbit remains circular.

5.2. Period Distribution of Inner Subsystems

The histogram of inner periods in solar-type hierarchies is plotted in Figure 1. It shows a marked difference with the period distribution of all field binaries, namely the excess of periods shorter than 30 days in inner subsystems. Preference of close binaries to be members of hierarchical systems is firmly established by prior work. For example, Tokovinin et al. (2006) determined that ∼80% of spectroscopic binaries with $P < 7$ days have tertiary companions. The statistical model of hierarchical multiplicity developed in (Tokovinin 2014a) matches the data quite well (after accounting for the selection), but underpredicts the fraction of inner subsystems with $P < 10$ days by a factor of two, because it does not account for correlation between close binaries and higher-order multiplicity. Recently Hwang et al. (2020) found that the occurrence rate of wide physical companions to eclipsing binaries is ∼3 times higher than for typical field stars (14.1% versus 4.5%).

The origin of the observed relation between close binaries and hierarchies is still under debate. The reader is referred to Moe & Kratter (2018) for a detailed analysis and an up-to-date population synthesis. The originally proposed mechanism of Lidov–Kozai cycles in misaligned triples acting in combination with tidal friction can account only for a minor fraction of the close subsystems, and its predictions disagree with reality. Specifically, the predicted excess of inner periods just below the tidal cutoff at $P < 10$ days and the concentration of mutual inclinations near 40° are not seen. Instead, there is no discontinuity in the distribution of inner periods at $P \sim 10$ days, but their numbers drop at $P > 30$ days (Figure 1). Moe & Kratter (2018) argue that the main agent that shrinks inner periods should be associated with the accretion of gas during mass assembly. The observed frequency of inner twins with mass ratio $q > 0.95$ formed by accretion also drops sharply at $P > 30$ days (see Figure 4 in Tokovinin 2021). However, the key issue of relating accretion to the presence of tertiary companions is still unsettled. Further discussion of this topic is beyond the scope of this paper. The point here is to illustrate how new homogeneous data on hierarchies contribute to the study of their formation mechanisms.

6. Summary

Multiyear spectroscopic monitoring of inner subsystems in solar-type hierarchies has been undertaken to elucidate distributions of periods, eccentricities, and mass ratios. The targets were derived from the sample of solar-type stars within 67 pc with unknown inner periods and enlarged by additional, more distant hierarchies. Spectroscopic (and visual) orbits based on these data are reported in 10 papers. The main results are as follows.

1. A total of 102 spectroscopic orbits with periods ranging from fraction of a day to several years were determined. The coverage is reasonably complete up to $P \sim 1000$ days.
2. Monitoring with CHIRON revealed new, additional subsystems: several presumed triples in fact are quadruples of 2 + 2 or 3 + 1 hierarchy.
3. The Gaia NSS provides orbits for only a third of the CHIRON sample, and a substantial fraction of Gaia orbits in common with CHIRON have reduced RV amplitudes or other problems.
4. The distribution of inner periods based on this survey, literature, and Gaia (Figure 1), differs from the canonical log-normal period distribution in the field. Inner subsystems have a strong excess of periods shorter than 30 days. The logarithmic inner period distribution has a local minimum in the 30–100 days bin.
5. The period-eccentricity diagram of inner solar-type subsystems (Figure 3) shows an interesting structure. Statistical data on periods, eccentricities, and mass ratios in these hierarchies will help in the development and verification of their formation models.

In a broader context, this study fits into the vast landscape of observational characterization of stellar hierarchies. Large photometric surveys designed for the study of transiting exoplanets have opened a new window on unusual and rare compact hierarchies like triply eclipsing planar worlds (e.g., Rappaport et al. 2022) that challenge current formation theories. Gaia has revolutionized the census of solar neighborhood by revealing wide pairs of stars with an unprecedented completeness and their connection to close binaries (e.g., Hwang et al. 2020; Hwang 2023). New data highlight the diversity of stellar hierarchies (Tokovinin 2021) and provide insights on their formation (Offner et al. 2022).

The research was funded by the NSF's NOIRLab. This work used the SIMBAD service operated by Centre des Données Stellaires (Strasbourg, France), bibliographic references from the Astrophysics Data System maintained by SAO/NASA, and the Washington Double Star Catalog maintained at USNO. This work has made use of data from the European Space Agency (ESA) mission Gaia (https://www.cosmos.esa.int/gaia), processed by the Gaia Data Processing and Analysis Consortium (DPAC; https://www.cosmos.esa.int/web/gaia/dpac/consortium). Funding for the DPAC has been provided by national institutions, in particular the institutions participating in the Gaia Multilateral Agreement.

Facilities: CTIO:1.5 m, Gaia.

ORCID iDs

Andrei Tokovinin https://orcid.org/0000-0002-2084-0782

References

Bashi, D., Shahaf, S., Mazeh, T., et al. 2022, MNRAS, 517, 3888
Buder, S., Sharma, S., Kos, J., et al. 2021, MNRAS, 506, 150
Cui, X.-Q., Zhao, Y.-H., Chu, Y.-Q., et al. 2012, RAA, 12, 1197
D'Orazio, D. J., & Duffell, P. C. 2021, ApJL, 914, L21
Gaia Collaboration, Arenou, F., Babusiaux, C., et al. 2022, arXiv:2206.05595
Gaia Collaboration, Brown, A. G. A., Vallenari, A., et al. 2021, A&A, 649, A1
Gorynya, N. A., & Tokovinin, A. 2014, MNRAS, 441, 2316
Gorynya, N. A., & Tokovinin, A. 2018, MNRAS, 475, 1375
Hwang, H.-C. 2023, MNRAS, 518, 1750
Hwang, H.-C., Hamer, J. H., Zakamska, N. L., & Schlaufman, K. C. 2020, MNRAS, 497, 2250
Mazeh, T. 1990, AJ, 99, 675
Meibom, S., & Mathieu, R. D. 2005, ApJ, 620, 970
Moe, M., & Kratter, K. M. 2018, ApJ, 854, 44
Nordström, B., Mayor, M., Andersen, J., et al. 2004, A&A, 418, 989
Offner, S. S. R., Moe, M., Kratter, K. M., et al. 2022, arXiv:arXiv:2203.10066
Pourbaix, D., Arenou, F., Gavras, P., et al. 2022, Gaia Data Release 3 (Paris: ESA), https://gea.esac.esa.int/archive/documentation/GDR3/index.html
Pourbaix, D., Tokovinin, A. A., Batten, A. H., et al. 2004, A&A, 424, 727
Price-Whelan, A. M., Hogg, D. W., Rix, H.-W., et al. 2020, ApJ, 895, 2
Raghavan, D., McAlister, H. A., Henry, T. J., et al. 2010, ApJS, 190, 1
Rappaport, S. A., Borkovits, T., Gagliano, R., et al. 2022, MNRAS, 513, 4341
Tokovinin, A. 2014a, AJ, 147, 87

Tokovinin, A. 2014b, AJ, 147, 86
Tokovinin, A. 2015, AJ, 150, 177
Tokovinin, A. 2016a, AJ, 152, 11
Tokovinin, A. 2016b, AJ, 152, 10
Tokovinin, A. 2018a, ApJS, 235, 6
Tokovinin, A. 2018b, AJ, 156, 48
Tokovinin, A. 2018c, AJ, 156, 194
Tokovinin, A. 2019a, AJ, 157, 91
Tokovinin, A. 2019b, AJ, 158, 222
Tokovinin, A. 2020a, AJ, 159, 88
Tokovinin, A. 2020b, AJ, 160, 69
Tokovinin, A. 2021, Univ, 7, 352
Tokovinin, A. 2022, AJ, 163, 161
Tokovinin, A. 2023, AJ, 165, 160
Tokovinin, A., Fischer, D. A., Bonati, M., et al. 2013, PASP, 125, 1336
Tokovinin, A., Hartung, M., & Hayward, T. L. 2010, AJ, 140, 510
Tokovinin, A., Hartung, M., Hayward, T. L., & Makarov, V. V. 2012, AJ, 144, 7
Tokovinin, A., Thomas, S., Sterzik, M., & Udry, S. 2006, A&A, 450, 681
Tokovinin, A. A., & Gorynya, N. A. 2001, A&A, 374, 227
Tokovinin, A. A., & Gorynya, N. A. 2007, A&A, 465, 257
Tokovinin, A. A., & Smekhov, M. G. 2002, A&A, 382, 118
Torres, G., Latham, D. W., & Quinn, S. N. 2021, ApJ, 921, 117
Triaud, A. H. M. J., Martin, D. V., Ségransan, D., et al. 2017, A&A, 608, A129